Neurobiology of Aging 76 (2019) 115–124

Contents lists available at ScienceDirect

Neurobiology of Aging

journal homepage: www.elsevier.com/locate/neuaging

Gray and white matter changes in presymptomatic genetic frontotemporal dementia: a longitudinal MRI study

Jessica L. Panman [a,b], Lize C. Jiskoot [a,b], Mark J.R.J. Bouts [b,c], Lieke H.H. Meeter [a], Emma L. van der Ende [a,b], Jackie M. Poos [a,b], Rogier A. Feis [b,c,d], Anneke J.A. Kievit [e], Rick van Minkelen [e], Elise G.P. Dopper [a,b,f], Serge A.R.B. Rombouts [b,c,d], John C. van Swieten [a,g], Janne M. Papma [a,*]

[a] Department of Neurology, Erasmus Medical Center, Rotterdam, the Netherlands
[b] Department of Radiology, Leiden University Medical Center, Leiden, the Netherlands
[c] Institute of Psychology, Leiden University, Leiden, the Netherlands
[d] Leiden Institute for Brain and Cognition, Leiden University, Leiden, the Netherlands
[e] Department of Clinical Genetics, Erasmus Medical Center, Rotterdam, the Netherlands
[f] Department of Neurology, VU medical Center, Amsterdam, the Netherlands
[g] Department of Clinical Genetics, VU Medical Center, Amsterdam, the Netherlands

ARTICLE INFO

Article history:
Received 16 July 2018
Received in revised form 19 December 2018
Accepted 27 December 2018
Available online 7 January 2019

Keywords:
Frontotemporal dementia
Magnetic resonance imaging
Diffusion tensor imaging
Hereditary dementia
Preclinical disease
Frontotemporal lobar degeneration

ABSTRACT

In genetic frontotemporal dementia, cross-sectional studies have identified profiles of presymptomatic neuroanatomical loss for *C9orf72* repeat expansion, *MAPT*, and *GRN* mutations. In this study, we characterize longitudinal gray matter (GM) and white matter (WM) brain changes in presymptomatic frontotemporal dementia. We included healthy carriers of *C9orf72* repeat expansion (n = 12), *MAPT* (n = 15), *GRN* (n = 33) mutations, and related noncarriers (n = 53), that underwent magnetic resonance imaging at baseline and 2-year follow-up. We analyzed cross-sectional baseline, follow-up, and longitudinal GM and WM changes using voxel-based morphometry and cortical thickness analysis in SPM and tract-based spatial statistics in FSL. Compared with noncarriers, *C9orf72* repeat expansion carriers showed lower GM volume in the cerebellum and insula, and WM differences in the anterior thalamic radiation, at baseline and follow-up. *MAPT* mutation carriers showed emerging GM temporal lobe changes and longitudinal WM degeneration of the uncinate fasciculus. *GRN* mutation carriers did not show presymptomatic neurodegeneration. This study shows distinct presymptomatic cross-sectional and longitudinal patterns of GM and WM changes across *C9orf72* repeat expansion, *MAPT*, and *GRN* mutation carriers compared with noncarriers.

1. Introduction

Hereditary frontotemporal dementia (FTD) is a neurodegenerative disorder, predominantly caused by autosomal dominant genetic mutations in the *MAPT* and *GRN* genes or a repeat expansion in the *C9orf72* gene (Renton et al., 2011; Seelaar et al., 2011). Increasing evidence confirms the presence of pathophysiological and subsequent neuroanatomical changes in the presymptomatic stage of genetic FTD and amyotrophic lateral sclerosis (ALS) (Bertrand et al., 2018; Borroni et al., 2008; Caroppo et al., 2015; Cash et al., 2017; Dopper et al., 2014; Floeter et al., 2016; Jiskoot et al., 2016, 2018; Lee et al., 2017; Meeter et al., 2016, 2017, 2018; Papma et al., 2017; Pievani et al., 2014; Rohrer et al., 2015, 2013; Walhout et al., 2015; Whitwell et al., 2011a). Previous magnetic resonance imaging (MRI) studies have revealed gene-specific neuroimaging profiles in healthy carriers of pathogenic FTD mutations (hereafter referred as "presymptomatic mutation carriers") (Bertrand et al., 2018; Borroni et al., 2008; Caroppo et al., 2015; Cash et al., 2017; Dopper et al., 2014; Lee et al., 2017; Papma et al., 2017; Pievani et al., 2014; Rohrer et al., 2015; Walhout et al., 2015). In presymptomatic *MAPT* mutation carriers, lower gray matter (GM) volume in the anterior temporal lobes has been found (Cash et al., 2017; Rohrer et al., 2015), as well as lower fractional anisotropy (FA) in the white matter (WM) of the right uncinate fasciculus when using region of interest (ROI) analyses (Dopper et al., 2014). In

* Corresponding author at: Department of Neurology, Erasmus Medical Center Rotterdam, Ee2291a Dr Molewaterplein 40, 3015 GD Rotterdam, the Netherlands. Tel.: +31 10 704 38 28; fax: +31 10 704 47 21.
E-mail address: j.papma@erasmusmc.nl (J.M. Papma).

0197-4580/
https://doi.org/10.1016/j.neurobiolaging.2018.12.017

presymptomatic *GRN* mutation carriers, subtle GM differences in the insula, temporal, and frontal lobes were shown (Caroppo et al., 2015; Cash et al., 2017; Pievani et al., 2014; Rohrer et al., 2015) and WM differences in the uncinate fasciculus and inferior fronto-occipital fasciculus (Borroni et al., 2008; Dopper et al., 2014). Presymptomatic *C9orf72* repeat expansion carriers were characterized by lower GM volume of the insula, thalamus, and cerebellum (Bertrand et al., 2018; Cash et al., 2017; Lee et al., 2017; Papma et al., 2017; Rohrer et al., 2015) and cortical thinning of the temporal lobe (Walhout et al., 2015). These changes were already shown up to 25 years before estimated symptom onset (Rohrer et al., 2015). WM loss in presymptomatic *C9orf72* repeat expansion carriers included the corticospinal tract, anterior thalamic radiation, inferior longitudinal fasciculus, and the uncinate fasciculus (Bertrand et al., 2018; Papma et al., 2017).

Although cross-sectional MRI studies in presymptomatic FTD indicate that the disease process starts several years before clinical symptom onset, studies that examine longitudinal presymptomatic GM and WM changes in specific mutations are scarce (Rohrer et al., 2015; Schuster et al., 2015). Understanding longitudinal presymptomatic FTD–related brain changes is important, as it enables both the identification of vulnerable brain regions and the timeframe and progression of brain changes, with important implications for disease management and treatment (Schuster et al., 2015). Progression of GM and WM changes in presymptomatic FTD carriers may follow a gradual trajectory, similar to the presymptomatic stage of other neurodegenerative diseases like Alzheimer's disease (AD), shown in the Dominant Inherited Alzheimer Network study (Bateman et al., 2012; Benzinger et al., 2013; Kinnunen et al., 2018; Rohrer et al., 2015) but could also deviate from findings in AD. For example, remarkable early brain changes have been found in *C9orf72* repeat expansion carriers, which may indicate that *C9orf72* repeat expansion–associated pathology knows an early start and progresses in a very slow manner (Papma et al., 2017; Rohrer et al., 2015) or could even exist as a neurodevelopmental disorder (Lee et al., 2017; Walhout et al., 2015). On the other hand, previous research demonstrated that atrophy rates during the symptomatic stage of FTD are twice as high compared with patients with AD (Frings et al., 2014; Krueger et al., 2010; Whitwell, 2010), with the fastest atrophy rates in FTD-*GRN* patients (Whitwell et al., 2011b, 2015). An interesting issue therefore is whether *GRN* pathology spreads in the last years before symptom onset with a much faster, more explosive rate (Jiskoot et al., 2018; Meeter et al., 2016). In the present study, we aimed to investigate longitudinal GM and WM brain changes in the presymptomatic stage of FTD, with a specific focus on FTD genotypic patterns. Some previous studies have used voxel-based morphometry (VBM; Borroni et al., 2008; Cash et al., 2017; Dopper et al., 2014; Papma et al., 2017; Whitwell et al., 2011a) and others used cortical thickness estimation for GM analyses in presymptomatic FTD (Bertrand et al., 2018; Caroppo et al., 2015; Lee et al., 2017; Pievani et al., 2014; Walhout et al., 2015). In this study, we used both methods, and additional tract-based spatial statistics (TBSS) for diffusion tensor imaging (DTI) analysis, to grasp the full extent of presymptomatic GM and WM differences. Furthermore, in normal brain aging (Hutton et al., 2009), and Parkinson's disease (Gerrits et al., 2016), differences between results from VBM and cortical thickness in the same sample have been demonstrated, indicating that both methods could be complementary (Hutton et al., 2009; Gerrits et al., 2016). We performed a 2-year follow-up study in which we investigated cross-sectional and longitudinal structural neuroimaging profiles using whole brain VBM, cortical thickness analysis, and TBSS in presymptomatic *C9orf72* repeat expansion carriers, *GRN* or *MAPT* mutation carriers and noncarriers.

2. Methods

2.1. Study procedure

2.1.1. Study protocol and ethical approval

In the FTD Risk Cohort, we investigated first-degree relatives of FTD patients with one of the 3 major autosomal pathogenic mutations (*C9orf72, MAPT, GRN*), as previously described in our baseline study articles (Dopper et al., 2014; Papma et al., 2017). In this study, every 2 years, participants underwent MRI of the brain, neurological examination, and neuropsychological assessment (Jiskoot et al., 2016, 2018). Knowledgeable informants (e.g., spouses, siblings) completed questionnaires and were interviewed on changes in cognition and/or behavior. Genotyping was performed at the baseline study visit (Dopper et al., 2014; Papma et al., 2017). As a result, participants were labeled as either mutation carriers or noncarriers. All clinical investigators and participants were blinded for the participants' genetic status, unless participants underwent predictive testing. The FTD Risk Cohort study was approved by the Medical and Ethical Review Committee of the Erasmus Medical Center, and written informed consent has been obtained from all participants.

2.1.2. Subject inclusion

For the present study, we selected all presymptomatic participants, either mutation carriers or healthy noncarrier family members, with a baseline and 2-year follow-up MRI scan (n = 113). We defined participants as presymptomatic based on: (1) not fulfilling established criteria for possible FTD, primary progressive aphasia, or ALS (Gorno-Tempini et al., 2011; Ludolph et al., 2015; Rascovsky et al., 2011), (2) the absence of cognitive or behavioral disorders on extensive neuropsychological assessment or the Neuropsychiatric Inventory Questionnaire (NPI-Q) (Cummings, 1997), as described previously (Dopper et al., 2014; Jiskoot et al., 2016, 2018; Papma et al., 2017), (3) the absence of signs of motor neuron disease on neurological examination, (4) the presence of normal cognitive functioning and behavior as reported by the participant and knowledgeable informant. The Frontotemporal Dementia–Clinical Rating Scale sum of boxes, Mini-Mental State Examination (MMSE), and NPI-Q were reported as functional, cognitive, and behavioral screening instruments, respectively. The neuropsychological assessment included tests considering language, attention, executive functioning, memory, visuoconstruction, and social cognition, for specifics see Jiskoot et al. (2018) and appendix A.

2.1.3. MRI acquisition

All participants underwent 3T T1-weighted and DTI at baseline and 2-year follow-up using a standardized protocol (Philips Achieva–Philips Medical Systems, Best, the Netherlands). T1-weighted images were acquired with the following scanning parameters: repetition time = 9.8 ms, echo time = 4.6 ms, flip angle = 8°, 140 slices, voxel size = 0.88 × 0.88 × 1.20 mm^3. DTI was performed using single-shot echo planar imaging with 61 noncollinear gradient directions (1 b = 0, 60 b = 1000 s/mm^2, repetition time = 8250 ms, echo time = 80 ms, flip angle = 90°, 70 axial slices, voxel size = 2 × 2 × 2 mm^3). Although MRI sequence parameters were fixed over time, during follow-up, a routine software update by the manufacturer was installed at our MRI site, dated September 17, 2015 (Appendix B). MRI images were visually checked for gross neurological pathology and artifacts, and excluded from analysis when image quality proved insufficient.

2.2. Image preprocessing and analysis

2.2.1. Voxel-based morphometry

Whole-brain T1-weighted images were preprocessed using the longitudinal processing stream within the Computation Anatomy

Toolbox of the Statistical Parametric Mapping software (SPM12; the Wellcome Trust Center for Neuroimaging, London, UK) running in MATLAB (2016b) (Mathworks, Natick, MA, USA). First, longitudinal images from all subjects were rigidly aligned within-subjects and the images were segmented into GM and WM and cerebrospinal fluid based on tissue probability. Afterward, segmented tissue images were aligned to standard space. Using diffeomorphic image registration (DARTEL; Ashburner and Friston, 2000), we created a study-specific GM template in standard space, and GM segmentations from all subjects were warped and normalized to this template. After registration and normalization, GM images were smoothed using a full-width at half-maximum kernel of 8 mm to correct for individual brain differences. We performed cross-sectional VBM analysis of variance (ANOVA) at the baseline and follow-up to compare mutation groups (*C9orf72*, *GRN,* and *MAPT*) with noncarriers and with each other, at both time points separately. Follow-up GM volume images were subtracted from their corresponding baseline maps and a longitudinal ANOVA was performed to determine the amount of change in GM over time between groups (Dopper et al., 2016). Statistical analysis was performed using a full factorial model with age, sex, scanner update, and baseline total intracranial volume (TIV) as covariates. TIV in mm^3 was estimated through the segmentation and tissue volume calculation of the GM, WM, and cerebrospinal fluid. The statistical threshold was set at $p < 0.05$ at cluster level, corrected for multiple comparisons using familywise error (FWE). We also explored clusters showing trends toward significant difference at $p^{FWE} < 0.1$.

2.2.2. Cortical thickness

We extended the standard brain segmentation protocol from the Computation Anatomy Toolbox in SPM12, as mentioned previously, with surface-based cortical thickness estimation for baseline and follow-up images, using projection-based thickness (Dahnke et al., 2013). For statistical analysis, we used the same models as for the VBM analysis, and performed cross-sectional baseline and follow-up analyses to compare the effect of mutation group (*C9orf72*, *GRN*, *MAPT*) with noncarriers and each other. We performed an ANOVA with age, sex, and scanner update (for follow-up analysis) as covariates and thresholded at $p^{FWE} < 0.05$ at cluster level. We also explored clusters showing trends toward significant difference at $p^{FWE} < 0.1$. For the longitudinal analysis, follow-up cortical thickness images were subtracted from their corresponding baseline maps, and a longitudinal ANOVA was performed to determine the amount of change in thickness over time for each participant, also at $p^{FWE} < 0.05$, corrected for age, sex, and scanner update. However, as recommended, the cortical thickness analyses were not adjusted for baseline TIV (http://www.neuro.uni-jena.de/cat12/CAT12-Manual.pdf).

2.2.3. Tract-based spatial statistics

Diffusion-weighted images were preprocessed using TBSS (part of the FMRIB Software Library, Smith et al., 2004) as described previously (Dopper et al., 2014; Papma et al., 2017). We used the FMRIB58_FA–derived skeleton instead of a study-specific skeleton to allow for comparisons across the baseline, follow-up, and longitudinal analyses. Skeletonized FA and mean diffusivity (MD) images were fed into voxelwise group statistics for cross-sectional baseline and follow-up analyses to investigate the effect of mutation group. For the longitudinal analysis, follow-up FA and MD images were subtracted from their corresponding baseline maps to determine the amount of change in WM integrity over time for each participant and compared between groups with an ANOVA. Comparisons were performed using permutation-based testing (5000 permutations), with age, gender, the scanner update, and baseline TIV as covariates. The statistical threshold was set at $p^{FWE} < 0.05$.

2.3. Statistical analyses

Other statistical analyses were performed using SPSS Statistics 24.0 for Windows (SPSS Inc, Chicago, IL, USA). Group differences in sex were analyzed using Pearson χ^2 tests. Age at time of MRI scan was compared by means of one-way ANOVA. Because of a skewed distribution, the MMSE and NPI-Q scores were analyzed with a Kruskal-Wallis test. Composite cognitive domain scores for language, attention, executive functioning, memory, visuoconstruction, and social cognition were computed and evaluated between groups as described previously (Jiskoot et al., 2018) and reported in Appendix A. As the distribution of neuropsychological test data was predominantly skewed, we applied Kruskal-Wallis tests, with post hoc Mann-Whitney-U tests for composite cognitive domain scores. We applied a significance level of $p < 0.05$ with post hoc Bonferroni comparisons for all statistical analyses.

3. Results

3.1. Subjects

DNA sequencing assigned participants either to the *C9orf72* repeat expansion carrier (n = 12), *MAPT* mutation carrier (n = 15), *GRN* mutation carrier (n = 33), or, in the case of mutation-negative family members, to the noncarrier group (n = 53). One presymptomatic *MAPT* mutation carrier was excluded from GM analysis due to a large cerebellar cyst, and one presymptomatic *C9orf72* repeat expansion carrier was excluded due to registration and reconstruction errors. GM analysis was carried out in 11 *C9orf72* repeat expansion, 14 *MAPT*, and 33 *GRN* mutation carriers, and 53 noncarriers and WM analysis in 12 *C9orf72* repeat expansion, 14 *MAPT*, and 28 *GRN* mutation carriers, and 50 noncarriers. Nine subjects were excluded from WM analysis due to signal dropout (n = 6) and motion artifacts (n = 3) on the DTI scan. All participants were presymptomatic at both the baseline and follow-up visit, with Frontotemporal Dementia–Clinical Rating Scale sum of boxes = 0 at both time points (Table 1). An overview of demographic characteristics is presented in Table 1. *MAPT* mutation carriers were significantly younger than noncarriers and *GRN* mutation carriers. Other subject characteristics were similar across groups, including screening measures for clinical symptoms such as the MMSE and NPI-Q. None of the participants scored below 2 standard deviations on neuropsychological tests. At baseline, all groups performed similar on composite cognitive domains (Appendix A). At follow-up, *C9orf72* repeat expansion carriers and noncarriers performed significantly worse than *GRN* mutation carriers on social cognition (Appendix A).

3.2. C9orf72 *repeat expansion carriers versus noncarriers*

3.2.1. Gray matter

Cross-sectional VBM analysis at baseline showed lower GM volume in the cerebellum, insula, left frontal, and left planum temporale in *C9orf72* repeat expansion carriers compared with noncarriers (Fig. 1A, Appendix C.1), whereas cortical thickness analysis showed thinning in the right postcentral gyrus and a trend toward thinning of the left precentral gyrus (at $p^{FWE} = 0.060$). Cross-sectional VBM analysis at 2-year follow-up showed lower GM volume in *C9orf72* repeat expansion carriers compared with noncarriers in the thalamus, cerebellum, and several bilateral cortical regions, that is, orbitofrontal and insular cortices, and the postcentral gyrus (Fig. 1A, Appendix C.1). In addition, cortical thickness analysis showed cortical thinning in bilateral precentral gyrus and right superior parietal lobule in *C9orf72* repeat expansion carriers compared with noncarriers (Fig. 1B, Appendix C.2). Longitudinal VBM and cortical thickness analyses did not reveal any significant

Table 1
Demographic characterization

Variable	Noncarriers	*MAPT*	*GRN*	*C9orf72*	*p*-value
Subjects (male)	53 (24)	15 (9)	33 (11)	12 (2)	0.094
Mean age (SD)	50.72 (10.73)	41.77 (9.50)	52.10 (7.53)	49.70 (12.36)	0.010[a]
<35	3	2	0	1	
35–50	18	11	13	6	
50–65	29	1	18	4	
65+	3	1	2	1	
Baseline					
MMSE	29.13 (1.21)	29.47 (0.64)	29.09 (1.40)	29.58 (0.67)	0.657
NPI-Q	0.19 (0.54)	1.50 (3.75)	0.70 (1.42)	0.55 (1.21)	0.401
Follow-up					
MMSE	29.26 (1.23)	28.80 (2.11)	28.84 (1.57)	29.25 (0.96)	0.580
NPI-Q	0.42 (0.88)	2.08 (5.77)	0.18 (0.48)	1.18 (1.66)	0.128

Key: FTD-CDR, Frontotemporal Dementia–Clinical Rating Scale sum of boxes; MMSE, Mini-Mental State Examination; NPI-Q, Neuropsychiatric Inventory Questionnaire; SD, standard deviation.
Scores for MMSE and NPI-Q are presented as mean scores (SD).
[a] *MAPT* mutation carriers significantly younger than noncarriers and *GRN* mutation carriers.

changes in *C9orf72* repeat expansion carriers. Furthermore, there were no brain regions where noncarriers showed lower GM volume or cortical thinning compared with *C9orf72* carriers at the baseline, follow-up, or longitudinally.

3.2.2. White matter

Cross-sectional analyses at baseline revealed lower FA in *C9orf72* repeat expansion carriers in frontotemporal tracts compared with noncarriers, predominantly located in the bilateral corticospinal tract and anterior thalamic radiation, the right inferior fronto-occipital fasciculus, and superior longitudinal fasciculus (Fig. 2A, Appendix C.3) and higher MD in almost the entire skeleton when compared with noncarriers (Fig. 2B, Appendix C.3). At follow-up, we found lower FA and increased MD in the same tracts as baseline analyses, although to a lesser extent (Fig. 2B, Appendix C.3). We did not find any significant longitudinal changes in the WM (both

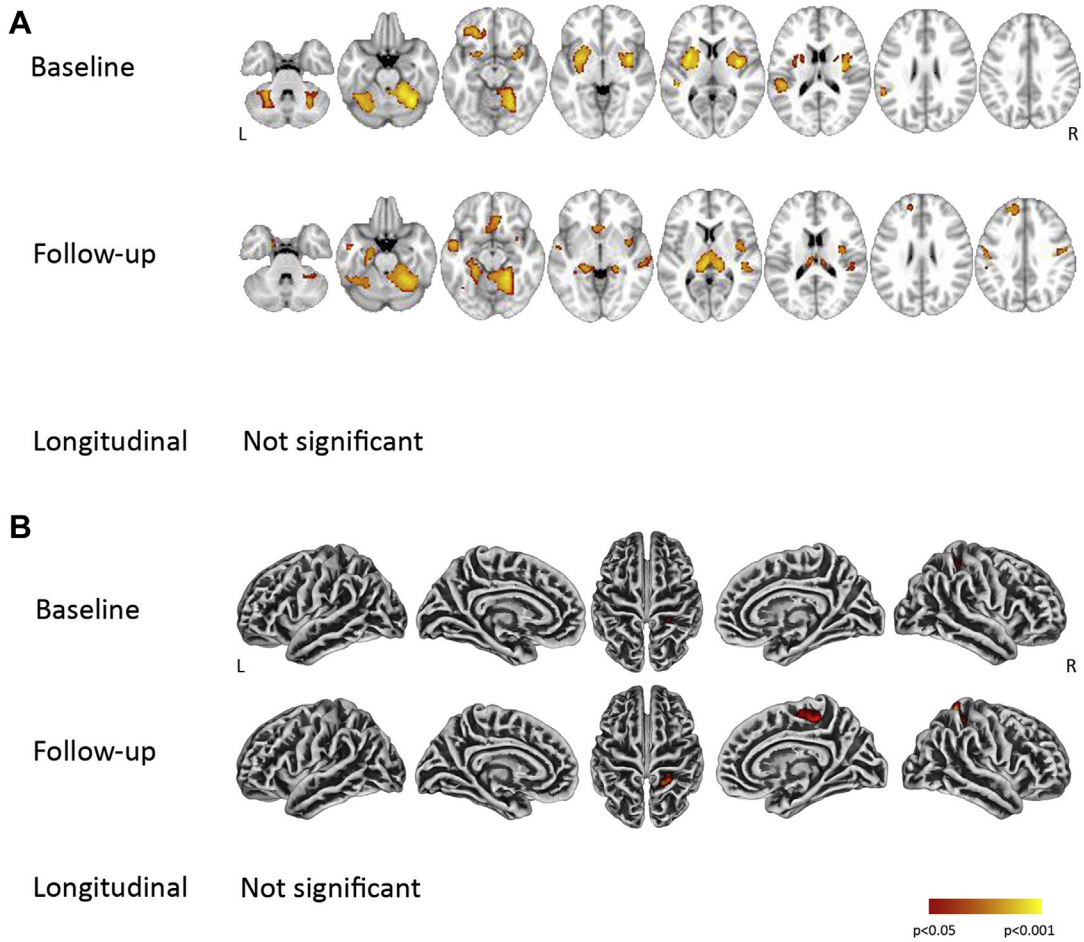

Fig. 1. – Gray matter differences in *C9orf72* repeat expansion carriers. (A) VBM comparisons, $p^{FWE} < 0.05$. GM of *C9orf72* repeat expansion carriers compared with noncarriers. (B) Cortical thickness analysis, $p^{FWE} < 0.05$. Thinning in *C9orf72* repeat expansion carriers compared with noncarriers. Abbreviations: GM, gray matter; VBM, voxel-based morphometry.

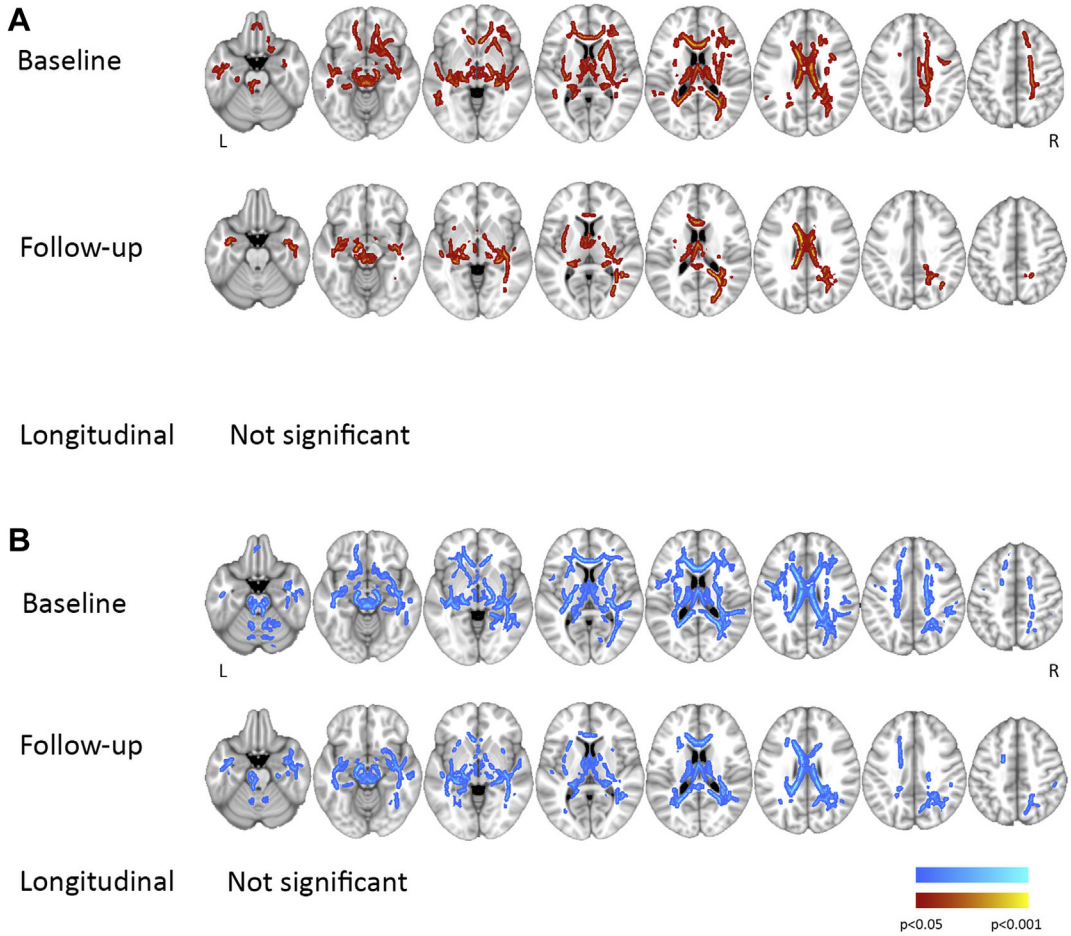

Fig. 2. White matter differences in *C9orf72* repeat expansion carriers. (A) Lower FA in *C9orf72* repeat expansion carriers compared with noncarriers, $p^{FWE} < 0.05$. (B) Higher MD in *C9orf72* repeat expansion carriers compared with noncarriers, $p^{FWE} < 0.05$. Abbreviations: FA, fractional anisotropy; MD, mean diffusivity.

FA and MD) of *C9orf72* repeat expansion carriers compared with noncarriers, or vice versa.

3.3. MAPT *mutation carriers versus noncarriers*

3.3.1. *Gray matter*

Cross-sectional VBM and cortical thickness analyses at baseline showed no GM volume differences in *MAPT* mutation carriers compared with noncarriers. VBM analysis at follow-up showed lower GM volume in the left temporal pole of *MAPT* mutation carriers (Fig. 3A, Appendix C.1), and cortical thickness analysis at follow-up showed a trend toward cortical thinning of the right inferior temporal lobe (at $p^{FWE} = 0.072$; Fig. 3B, Appendix C.2). Longitudinal VBM analysis showed significant GM volume decline in the hippocampus compared with noncarriers (Fig. 3A, Appendix C.1), whereas cortical thickness analysis did not pick up any longitudinal changes. Noncarriers did not show areas of GM volume decline or cortical thinning compared with *MAPT* mutation carriers.

3.3.2. *White matter*

Baseline or follow-up cross-sectional analyses did not show any significant WM differences between *MAPT* mutation carriers and noncarriers. Longitudinal analyses showed significant lower FA in the left uncinate fasciculus, the left anterior thalamic radiation, and the left inferior fronto-occipital fasciculus of *MAPT* mutation carriers compared with noncarriers (Fig. 4, Appendix C.3). There were no significant changes in MD over time between *MAPT* mutation carriers and noncarriers.

3.4. GRN *mutation carriers versus noncarriers*

GRN mutation carriers did not show GM volume or cortical thickness differences compared with noncarriers at baseline, follow-up, or in longitudinal analyses. In addition, noncarriers did not show any loss of GM volume or cortical thinning compared with *GRN* mutation carriers. Furthermore, we did not find significant differences in FA or MD between *GRN* mutation carriers and noncarriers.

3.5. *Comparisons between mutation groups*

3.5.1. *Gray matter*

C9orf72 repeat expansion carriers showed lower GM volume in the cerebellum, thalamus, and insula at both baseline and follow-up when compared with *MAPT* mutation carriers (Appendix C.1). Compared with *GRN* mutation carriers, *C9orf72* repeat expansion carriers had lower GM volume in the cerebellum, thalamus, insula, and frontal cortical regions at baseline and follow-up (Appendix C.1). In addition, cortical thickness analyses showed thinning in *C9orf72* repeat expansion carriers compared with *GRN* mutation carriers in the precentral and postcentral gyrus, at baseline and follow-up (Appendix C.2). We did not find longitudinal VBM or cortical thickness changes in *C9orf72* repeat expansion carriers

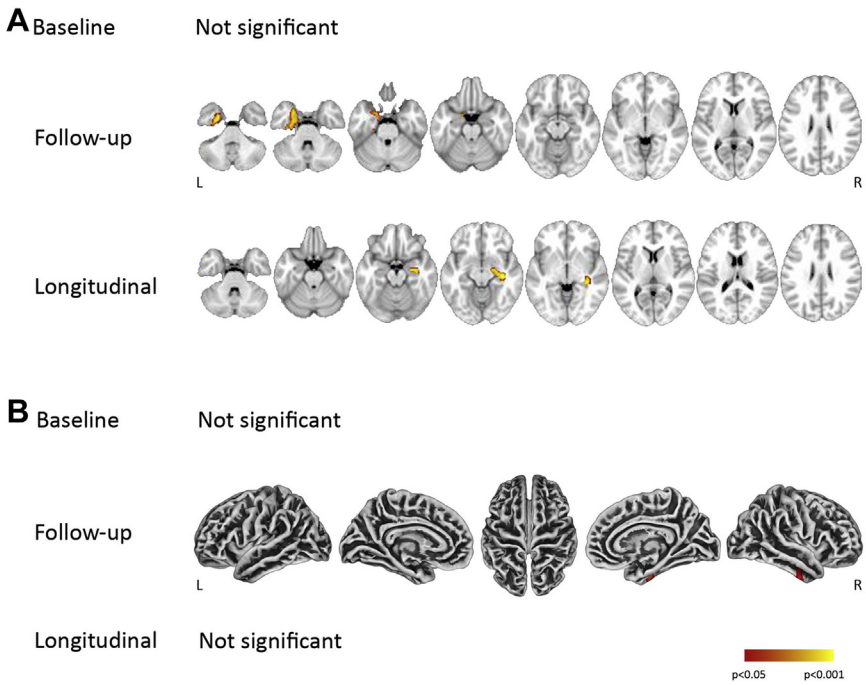

Fig. 3. Gray matter changes in *MAPT* mutation carriers. (A) VBM comparisons, $p^{FWE} < 0.05$. GM of *MAPT* mutation carriers compared with noncarriers. (B) Cortical thickness analysis, $p^{FWE} < 0.05$. Thinning in *MAPT* mutation carriers compared with noncarriers. Abbreviations: GM, gray matter; VBM, voxel-based morphometry.

compared with *GRN* or *MAPT* mutation carriers. We found thinning of the right temporal pole in *MAPT* mutation carriers compared with *GRN* mutation carriers at the follow-up (Appendix C.2) but not at baseline or longitudinally. There were no VBM or cortical thickness changes in *MAPT* mutation carriers compared with *C9orf72* repeat expansion carriers or changes in *GRN* mutation carriers compared with *MAPT* mutation carriers or *C9orf72* repeat expansion carriers at baseline, follow-up, or longitudinally.

3.5.2. White matter

C9orf72 repeat expansion carriers had lower FA and higher MD in the bilateral anterior thalamic radiation and forceps minor and major, right uncinate, and inferior fronto-occipital fasciculus and corticospinal tract at baseline compared with *MAPT* mutation carriers (Appendix C.3). At follow-up, *C9orf72* repeat expansion carriers had lower FA in the bilateral anterior thalamic radiation, right temporal tract, and left frontal tract compared with *MAPT* mutation carriers, without differences in MD at follow-up. Compared with *GRN* mutation carriers, we found higher MD in *C9orf72* repeat expansion carriers in bilateral temporal and parietal tracts at baseline and in the right superior longitudinal and inferior fronto-occipital fasciculus at follow-up (Appendix C.3). We did not find differences in FA between *C9orf72* repeat expansion carriers and *GRN* mutation carriers. Longitudinal analysis did not reveal any significant differences in FA or MD between *C9orf72* repeat expansion carriers and *MAPT* or *GRN* mutation carriers. Compared with *GRN* mutation carriers, we found a longitudinal decline of FA in *MAPT* mutation carriers in left frontal tracts, predominantly in the uncinate and inferior fronto-occipital fasciculus (Appendix C.3) No other FA or MD changes were found in *MAPT* mutation carriers at baseline or follow-up compared with *GRN* mutation carriers or *C9orf72* repeat expansion carriers. Compared with *MAPT* mutation carriers, *GRN* mutation carriers had lower FA at follow-up in left frontal tracts, predominantly the forceps major, but not at baseline or longitudinal analyses (Appendix C.3). We did not find changes in FA or MD in *GRN* mutation carriers compared with *C9orf72* repeat expansion carriers.

4. Discussion

In this longitudinal MRI study, we found presymptomatic GM and WM changes in *C9orf72* repeat expansion carriers and *MAPT* mutation carriers at cross-sectional and longitudinal analyses, but not in *GRN* mutation carriers. Compared with noncarriers, presymptomatic *C9orf72* repeat expansion carriers showed prominent lower GM volume in the cerebellum, thalamus, insula, and cortical frontal and temporal regions, seemingly stable over time. WM differences in *C9orf72* repeat expansion carriers were found in subcortical and posterior tracts, particularly the anterior thalamic radiation. *MAPT* mutation carriers were characterized by left-sided GM volume loss and right-sided cortical thinning in the temporal

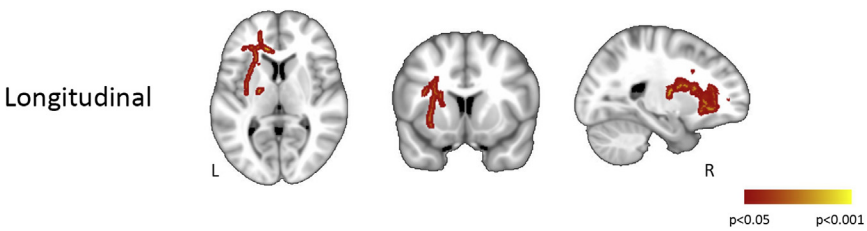

Fig. 4. Longitudinal FA degeneration in *MAPT* mutation carriers compared with noncarriers, $p^{FWE} < 0.05$. Abbreviation: FA, fractional anisotropy.

lobe at follow-up, and longitudinal WM changes in predominantly left-sided frontotemporal tracts when compared with noncarriers.

Our longitudinal findings indicate that the presymptomatic stage of *C9orf72* repeat expansion is characterized by a stable lower GM volume in the cerebellum, thalamus, insula, and several frontal and temporal regions (Rohrer et al., 2015). The prominent cerebellar atrophy was in line with other presymptomatic cross-sectional studies (Bertrand et al., 2018; Cash et al., 2017; Papma et al., 2017), although the study of Rohrer et al. suggested a temporal ordering of presymptomatic changes with atrophy in the thalamus, insula, occipital, frontal, and temporal lobe preceding cerebellar atrophy, already 25 years before estimated symptom onset (Rohrer et al., 2015). Due to methodological differences (e.g., mixed effect models based on ROI data vs. whole-brain analyses, percentage of TIV vs. absolute measures, and the use of estimated years of onset), it is difficult to compare our findings to the GENFI consortium article. However, it is important to appreciate the fact that *C9orf72* repeat expansion mutation carriers seem to show remarkable early GM changes (Bertrand et al., 2018; Rohrer et al., 2015; Walhout et al., 2015). This has been explained previously as either following a trajectory with an early onset and very slow progression of atrophy (Rohrer et al., 2015) or as a neurodevelopmental disorder (Lee et al., 2017; Walhout et al., 2015). Although our results agree with early GM and WM differences in presymptomatic *C9orf72* repeat expansion carriers compared with noncarriers, we cannot comment on the underlying mechanism. Stable lower GM volume may indicate a neurodevelopmental process but could also mean that our 2-year follow-up period is not sufficient to detect very slow progressive brain changes.

Our findings of extensive subcortical WM differences at baseline between *C9orf72* repeat expansion carriers and noncarriers are in line with previous studies, indicating early involvement of the thalamic radiation in symptomatic *C9orf72* carriers, with both the ALS and FTD phenotype (Bede et al., 2013; Mahoney et al., 2012; Schonecker et al., 2018). Furthermore, in this study, we showed that these WM differences remain relatively stable during a 2-year period. Functional connectivity loss in presymptomatic *C9orf72* repeat expansion carriers has been found in the thalamus and the salience network (Lee et al., 2017). Decreasing WM connections in the thalamus in *C9orf72* repeat expansion may underlie functional connectivity and neuronal loss in areas related to the salience network, such as the insula and orbitofrontal cortex (Seeley, 2010; Uddin, 2015), which is strongly associated with FTD (Seeley, 2010; Zhou et al., 2010).

The GM and WM regions that were affected in our cross-sectional analyses in *C9orf72* repeat expansion carriers were in accordance with expected pathology in FTD and ALS (Floeter et al., 2016), for example, orbitofrontal, temporal, and insula atrophy are associated with behavioral variant FTD (Gordon et al., 2016; Meeter et al., 2017; Seelaar et al., 2011), and changes in the precentral and postcentral gyri may eventually underlie ALS (Chio et al., 2014; Turner et al., 2012). Our results of subcortical WM loss could well fit both FTD and ALS phenotypes of the *C9orf72* repeat expansion (Bede et al., 2013; Mahoney et al., 2012; Schonecker et al., 2018). When performing MRI group analysis in specifically presymptomatic *C9orf72* repeat expansion carriers, it is important to keep in mind the heterogeneity in the disease phenotype, for example, FTD or ALS, memory or psychiatric disorders (Floeter et al., 2016). In line with this reasoning, the location of emerging presymptomatic GM volume loss might predict the disease phenotype of an individual *C9orf72* repeat expansion carrier. And, both the onset of pathophysiological changes and the affected brain regions may be highly variable across patients, which complicates comparisons between cross-sectional group analyses and claims on the onset of neurodegeneration. The mean disease onset in *C9orf72* repeat expansion carriers has been reported at 50 years of age, ranging from early adulthood to old age, from 27 to 83 years, and large intrafamily heterogeneity in disease onset and phenotype is common (Olszewska et al., 2016; Van Mossevelde et al., 2017). Therefore, the disease trajectory of *C9orf72* repeat expansion carriers may be elucidated by longer follow-up periods and longitudinal modeling with both presymptomatic and symptomatic carriers with different phenotypes.

At follow-up, we found cortical GM thinning in the right temporal lobe in presymptomatic *MAPT* mutation carriers and GM volume loss in the left temporal pole and parahippocampal gyrus, which is line with previous cross-sectional presymptomatic *MAPT* studies (Cash et al., 2017; Dopper et al., 2014; Rohrer et al., 2015), and resembles the atrophy pattern found in symptomatic *MAPT* carriers (Gordon et al., 2016; Rohrer et al., 2010; Whitwell et al., 2012, 2015). Furthermore, GM volume in the right hippocampus significantly decreased over time. In addition, we found longitudinal WM changes in left-sided frontotemporal association tracts including the uncinate fasciculus, which connects structures of the limbic system in the temporal lobe with the orbitofrontal cortex and has been indicated to underlie inhibition and impulse control (Hornberger et al., 2011; Olson et al., 2015). Although our results are somewhat contradicting in asymmetry, and involve left or right hemispheres in VBM and cortical thickness analyses, this may suggest emerging pathophysiological changes in both temporal lobes of *MAPT* mutation carriers. Therefore, as previously proposed, VBM and cortical thickness analyses may be applied as complementary methods (Hutton et al., 2009; Gerrits et al., 2016). VBM relies on a mixture of measurements in cortical thickness, cortical surface areas, and folding of the gyri (Ashburner and Friston, 2000). When used together, voxel-based cortical thickness analysis could aid understanding of underlying GM differences, especially in age-related brain changes (Hutton et al., 2009; Pereira et al., 2012). Although the *MAPT* mutation carriers were younger (mean age: 41.77) than noncarriers (mean age: 50.72) and *GRN* mutation carriers (mean age: 52.10), mean onset in *MAPT* mutations has been reported at 55 (Olszewska et al., 2016) and ranges till before 40 in some families (Seelaar et al., 2011). Therefore, most of our *MAPT* mutation carriers are likely to be within 1 or 2 decades before symptom onset. Our present findings combined with previous functional MRI, cognitive, and GM studies (Jiskoot et al., 2016; Rohrer et al., 2015; Whitwell et al., 2011a), indicate that GM and WM loss in presymptomatic *MAPT* carriers gradually progressed in a period of 5 to 10 years before symptom onset, starting in the temporal lobe, followed by slowly progressive cognitive decline.

The absence of any significant changes in a relatively large cohort of presymptomatic *GRN* mutation carriers compared with noncarriers in the present study is a remarkable finding, supported by previous cross-sectional studies (Cash et al., 2017; Dopper et al., 2014). One may argue that in a voxel-based groupwise analysis, subtle changes may remain undetected due to the typical, but in the presymptomatic stage, not yet visible asymmetrical left- or right-sided atrophy in *GRN* mutation carriers (Cash et al., 2017; Rohrer et al., 2010). Yet, Rohrer et al. found GM volume decline 15 years before expected age of onset with linear mixed modeling in *GRN* mutation carriers when combining the right insula and left insula (Rohrer et al., 2015). An alternative explanation might be that pathophysiological changes due to *GRN* mutation carriers spread quite rapidly, with extensive damage in a short period before symptom onset (Cash et al., 2017). Such hypothesis may be supported by the rapid decrease in cognitive functioning and strong increase in cerebrospinal fluid NfL levels in the short transitional stage from presymptomatic till symptom onset in *GRN* mutation carriers (Jiskoot et al., 2018; Meeter et al, 2016, 2017, 2018; Rohrer et al., 2008), accompanied by quickly expanding atrophy on

T1-weighted imaging, starting 18 months before symptom onset (Rohrer et al., 2008). Because the asymmetric left- or right-sided pattern of atrophy differs in patients even from the same families (Gordon et al., 2016; van Swieten and Heutink, 2008; Whitwell et al., 2012), and therefore groupwise neuroimaging analyses in presymptomatic carriers may result in a less useful biomarker for *GRN* mutation carriers, other biomarkers that measure pathological changes may be necessary. In *GRN* mutation carriers, mean symptom onset may be 65 years but fluctuates within families up to 20 years (Olszewska et al., 2016; Seelaar et al., 2011). Rapid changes over time implicate that 6- to 12 months monitoring from susceptible ages, for example, from ~45 years onward may be indicated in *GRN* mutation carriers (Onyike and Diehl-Schmid, 2013; Seelaar et al., 2011; van Swieten and Heutink, 2008) to enable prescription of—future—pharmacological treatment before onset of the neurodegenerative process.

Key strengths of our study are the longitudinal measurements in a large cohort of presymptomatic FTD mutation carriers and the single-center standardized MRI protocol with stable sequence parameters over time. Longitudinal multimodal imaging adds significant value over cross-sectional or unimodal imaging, as it enables insight into the profile and trajectory of brain changes. However, our current cross-sectional baseline findings in *C9orf72* repeat expansion carriers were not completely compliant with previous baseline findings of our group (Papma et al., 2017), and can be explained by the current increased control group that could have led to an increase in statistical power. Especially for the *C9orf72* repeat expansion and *MAPT* mutation group, our sample size was quite small, and results in these mutation groups may have been driven by individual carriers. ROI analyses could overcome some of the power problems, as it significantly reduces the strictness of the multiple comparisons correction, however, with the risk that unexpected brain regions may be overlooked. Before choosing predefined ROIs, explorative whole-brain analyses in the presymptomatic stage are necessary, which we aimed to accomplish with our present study. Furthermore, when using mixed-effects models and longer follow-up periods, ROI-based analysis could elucidate on the rate of brain changes and the acceleration related to time toward symptom onset or increasing age, as, for example, in the GENFI study (Rohrer et al., 2015). However, using estimated years to onset in longitudinal mixed-effects models may be disadvantageous, as large intrafamiliar heterogeneity in age at disease onset has been reported in genetic FTD mutations (Olszewska et al., 2016, Seelaar et al., 2011; Van Mossevelde et al., 2017). Our follow-up and longitudinal results may have been slightly compromised by a software upgrade on our MRI scanner (Shuter et al., 2008; Takao et al., 2012, 2013). To account for possible signal changes, we added a covariate to our statistical analyses, minimizing the potential effects of the scanner update.

In conclusion, this study shows distinct presymptomatic GM and WM alterations across *C9orf72* repeat expansion and *MAPT* and *GRN* mutations carriers. Presymptomatic neuroanatomical changes in *C9orf72* repeat expansion carriers, in particular, affecting the cerebellum and subcortical GM and WM, may be present early in the disease process, and our results point toward a possible neurodevelopmental disorder. In *MAPT* mutation carriers, our results suggest gradual progression of neurodegeneration, starting with GM volume loss, cortical thinning, and WM integrity loss in the temporal lobes. Rapid pathophysiological and neuroanatomical progression may reflect the trajectory before symptom onset in *GRN* mutation carriers, as we found no cross-sectional and longitudinal changes in a relatively large group of presymptomatic *GRN* mutation carriers. Complicating factors when performing longitudinal group analyses in presymptomatic FTD mutation carriers are an asymmetric pattern of atrophy and heterogeneity in pathophysiology, phenotype, and onset age. Other studies may confirm and elaborate on our longitudinal findings, increasing insight in the timing and progression of genotype- and phenotype-related presymptomatic neurodegeneration in genetic FTD.

Disclosure

The authors report no conflicts of interest.

Acknowledgements

The authors would like to thank all the participants and their families for taking part in this study.

This work has received financial support from Dioraphte Foundation grant 09-02-00, the Association for frontotemporal Dementias Research Grant 2009, The Netherlands organization for Scientific Research (NWO) grant HCMI 056-13-018, ZonMw Memorabel project number 733050103 and 733050813, the Bluefield project, JPND PreFrontAls consortium project number 733051042, and Alzheimer Nederland project WE.09-2014-4 for LHHM. SARBR and MJRJB were supported by NWO-Vici grant 016-130-677.

Appendix A. Supplementary data

Supplementary data associated with this article can be found, in the online version, at https://doi.org/10.1016/j.neurobiolaging.2018.12.017.

References

Ashburner, J., Friston, K.J., 2000. Voxel-based morphometry–the methods. Neuroimage 11 (6 Pt 1), 805–821.

Bateman, R.J., Xiong, C., Benzinger, T.L., Fagan, A.M., Goate, A., Fox, N.C., Marcus, D.S., Cairns, N.J., Xie, X., Blazey, T.M., Holtzman, D.M., Santacruz, A., Buckles, V., Oliver, A., Moulder, K., Aisen, P.S., Ghetti, B., Klunk, W.E., McDade, E., Martins, R.N., Masters, C.L., Mayeux, R., Ringman, J.M., Rossor, M.N., Schofield, P.R., Sperling, R.A., Salloway, S., Morris, J.C., Dominantly Inherited Alzheimer, Network, 2012. Clinical and biomarker changes in dominantly inherited Alzheimer's disease. N. Engl. J. Med. 367, 795–804.

Bede, P., Bokde, A.L., Byrne, S., Elamin, M., McLaughlin, R.L., Kenna, K., Fagan, A.J., Pender, N., Bradley, D.G., Hardiman, O., 2013. Multiparametric MRI study of ALS stratified for the C9orf72 genotype. Neurology 81, 361–369.

Benzinger, T.L., Blazey, T., Jack Jr., C.R., Koeppe, R.A., Su, Y., Xiong, C., Raichle, M.E., Snyder, A.Z., Ances, B.M., Bateman, R.J., Cairns, N.J., Fagan, A.M., Goate, A., Marcus, D.S., Aisen, P.S., Christensen, J.J., Ercole, L., Hornbeck, R.C., Farrar, A.M., Aldea, P., Jasielec, M.S., Owen, C.J., Xie, X., Mayeux, R., Brickman, A., McDade, E., Klunk, W., Mathis, C.A., Ringman, J., Thompson, P.M., Ghetti, B., Saykin, A.J., Sperling, R.A., Johnson, K.A., Salloway, S., Correia, S., Schofield, P.R., Masters, C.L., Rowe, C., Villemagne, V.L., Martins, R., Ourselin, S., Rossor, M.N., Fox, N.C., Cash, D.M., Weiner, M.W., Holtzman, D.M., Buckles, V.D., Moulder, K., Morris, J.C., 2013. Regional variability of imaging biomarkers in autosomal dominant Alzheimer's disease. Proc. Natl. Acad. Sci. U. S. A. 110, E4502–E4509.

Bertrand, A., Wen, J., Rinaldi, D., Houot, M., Sayah, S., Camuzat, A., Fournier, C., Fontanella, S., Routier, A., Couratier, P., Pasquier, F., Habert, M.O., Hannequin, D., Martinaud, O., Caroppo, P., Levy, R., Dubois, B., Brice, A., Durrleman, S., Colliot, O., Le Ber, I., Predict to Prevent Frontotemporal Lobar Degeneration and Amyotrophic Lateral Sclerosis (PREV-DEMALS) Study Group, 2018. Early cognitive, structural, and microstructural changes in presymptomatic C9orf72 carriers younger than 40 years. JAMA Neurol. 75, 236–245.

Borroni, B., Alberici, A., Premi, E., Archetti, S., Garibotto, V., Agosti, C., Gasparotti, R., Di Luca, M., Perani, D., Padovani, A., 2008. Brain magnetic resonance imaging structural changes in a pedigree of asymptomatic progranulin mutation carriers. Rejuvenation Res. 11, 585–595.

Caroppo, P., Habert, M.O., Durrleman, S., Funkiewiez, A., Perlbarg, V., Hahn, V., Bertin, H., Gaubert, M., Routier, A., Hannequin, D., Deramecourt, V., Pasquier, F., Rivaud-Pechoux, S., Vercelletto, M., Edouart, G., Valabregue, R., Lejeune, P., Didic, M., Corvol, J.C., Benali, H., Lehericy, S., Dubois, B., Colliot, O., Brice, A., Le Ber, I., Predict-PGRN study group, 2015. Lateral temporal lobe: an early imaging marker of the presymptomatic GRN disease? J. Alzheimers Dis. 47, 751–759.

Cash, D.M., Bocchetta, M., Thomas, D.L., Dick, K.M., van Swieten, J.C., Borroni, B., Galimberti, D., Masellis, M., Tartaglia, M.C., Rowe, J.B., Graff, C., Tagliavini, F., Frisoni, G.B., Laforce Jr., R., Finger, E., de Mendonca, A., Sorbi, S., Rossor, M.N., Ourselin, S., Rohrer, J.D., Genetic FTD Initiative, GENFI, 2017. Patterns of gray

matter atrophy in genetic frontotemporal dementia: results from the GENFI study. Neurobiol. Aging 62, 191–196.
Chio, A., Pagani, M., Agosta, F., Calvo, A., Cistaro, A., Filippi, M., 2014. Neuroimaging in amyotrophic lateral sclerosis: insights into structural and functional changes. Lancet Neurol. 13, 1228–1240.
Cummings, J.L., 1997. The Neuropsychiatric Inventory: assessing psychopathology in dementia patients. Neurology 48 (5 Suppl 6), S10–S16.
Dahnke, R., Yotter, R.A., Gaser, C., 2013. Cortical thickness and central surface estimation. Neuroimage 65, 336–348.
Dopper, E.G., Chalos, V., Ghariq, E., den Heijer, T., Hafkemeijer, A., Jiskoot, L.C., de Koning, I., Seelaar, H., van Minkelen, R., van Osch, M.J., Rombouts, S.A., van Swieten, J.C., 2016. Cerebral blood flow in presymptomatic MAPT and GRN mutation carriers: a longitudinal arterial spin labeling study. Neuroimage Clin. 12, 460–465.
Dopper, E.G., Rombouts, S.A., Jiskoot, L.C., den Heijer, T., de Graaf, J.R., de Koning, I., Hammerschlag, A.R., Seelaar, H., Seeley, W.W., Veer, I.M., van Buchem, M.A., Rizzu, P., van Swieten, J.C., 2014. Structural and functional brain connectivity in presymptomatic familial frontotemporal dementia. Neurology 83, e19–e26.
Floeter, M.K., Bageac, D., Danielian, L.E., Braun, L.E., Traynor, B.J., Kwan, J.Y., 2016. Longitudinal imaging in C9orf72 mutation carriers: relationship to phenotype. Neuroimage Clin. 12, 1035–1043.
Frings, L., Yew, B., Flanagan, E., Lam, B.Y., Hull, M., Huppertz, H.J., Hodges, J.R., Hornberger, M., 2014. Longitudinal grey and white matter changes in frontotemporal dementia and Alzheimer's disease. PLoS One 9, e90814.
Gerrits, N.J., van Loenhoud, A.C., van den Berg, S.F., Berendse, H.W., Foncke, E.M., Klein, M., Stoffers, D., van der Werf, Y.D., van den Heuvel, O.A., 2016. Cortical thickness, surface area and subcortical volume differentially contribute to cognitive heterogeneity in Parkinson's disease. PLoS One 11, e0148852.
Gordon, E., Rohrer, J.D., Fox, N.C., 2016. Advances in neuroimaging in frontotemporal dementia. J. Neurochem. 138 (Suppl 1), 193–210.
Gorno-Tempini, M.L., Hillis, A.E., Weintraub, S., Kertesz, A., Mendez, M., Cappa, S.F., Ogar, J.M., Rohrer, J.D., Black, S., Boeve, B.F., Manes, F., Dronkers, N.F., Vandenberghe, R., Rascovsky, K., Patterson, K., Miller, B.L., Knopman, D.S., Hodges, J.R., Mesulam, M.M., Grossman, M., 2011. Classification of primary progressive aphasia and its variants. Neurology 76, 1006–1014.
Hornberger, M., Geng, J., Hodges, J.R., 2011. Convergent grey and white matter evidence of orbitofrontal cortex changes related to disinhibition in behavioural variant frontotemporal dementia. Brain 134 (Pt 9), 2502–2512.
Hutton, C., Draganski, B., Ashburner, J., Weiskopf, N., 2009. A comparison between voxel-based cortical thickness and voxel-based morphometry in normal aging. Neuroimage 48, 371–380.
Jiskoot, L.C., Dopper, E.G., Heijer, T., Timman, R., van Minkelen, R., van Swieten, J.C., Papma, J.M., 2016. Presymptomatic cognitive decline in familial frontotemporal dementia: a longitudinal study. Neurology 87, 384–391.
Jiskoot, L.C., Panman, J.L., van Asseldonk, L., Franzen, S., Meeter, L.H.H., Donker Kaat, L., van der Ende, E.L., Dopper, E.G.P., Timman, R., van Minkelen, R., van Swieten, J.C., van den Berg, E., Papma, J.M., 2018. Longitudinal cognitive biomarkers predicting symptom onset in presymptomatic frontotemporal dementia. J. Neurol. 265, 1381–1392.
Kinnunen, K.M., Cash, D.M., Poole, T., Frost, C., Benzinger, T.L.S., Ahsan, R.L., Leung, K.K., Cardoso, M.J., Modat, M., Malone, I.B., Morris, J.C., Bateman, R.J., Marcus, D.S., Goate, A., Salloway, S.P., Correia, S., Sperling, R.A., Chhatwal, J.P., Mayeux, R.P., Brickman, A.M., Martins, R.N., Farlow, M.R., Ghetti, B., Saykin, A.J., Jack Jr., C.R., Schofield, P.R., McDade, E., Weiner, M.W., Ringman, J.M., Thompson, P.M., Masters, C.L., Rowe, C.C., Rossor, M.N., Ourselin, S., Fox, N.C., Dominantly Inherited Alzheimer Network, 2018. Presymptomatic atrophy in autosomal dominant Alzheimer's disease: a serial magnetic resonance imaging study. Alzheimers Dement. 14, 43–53.
Krueger, C.E., Dean, D.L., Rosen, H.J., Halabi, C., Weiner, M., Miller, B.L., Kramer, J.H., 2010. Longitudinal rates of lobar atrophy in frontotemporal dementia, semantic dementia, and Alzheimer's disease. Alzheimer Dis. Assoc. Disord. 24, 43–48.
Lee, S.E., Sias, A.C., Mandelli, M.L., Brown, J.A., Brown, A.B., Khazenzon, A.M., Vidovszky, A.A., Zanto, T.P., Karydas, A.M., Pribadi, M., Dokuru, D., Coppola, G., Geschwind, D.H., Rademakers, R., Gorno-Tempini, M.L., Rosen, H.J., Miller, B.L., Seeley, W.W., 2017. Network degeneration and dysfunction in presymptomatic C9ORF72 expansion carriers. Neuroimage Clin. 14, 286–297.
Ludolph, A., Drory, V., Hardiman, O., Nakano, I., Ravits, J., Robberecht, W., Shefner, J., WFN Research Group On ALS/MND, 2015. A revision of the El Escorial criteria - 2015. Amyotroph. Lateral Scler. Frontotemporal Degener. 16, 291–292.
Mahoney, C.J., Beck, J., Rohrer, J.D., Lashley, T., Mok, K., Shakespeare, T., Yeatman, T., Warrington, E.K., Schott, J.M., Fox, N.C., Rossor, M.N., Hardy, J., Collinge, J., Revesz, T., Mead, S., Warren, J.D., 2012. Frontotemporal dementia with the C9ORF72 hexanucleotide repeat expansion: clinical, neuroanatomical and neuropathological features. Brain 135 (Pt 3), 736–750.
Meeter, L.H., Dopper, E.G., Jiskoot, L.C., Sanchez-Valle, R., Graff, C., Benussi, L., Ghidoni, R., Pijnenburg, Y.A., Borroni, B., Galimberti, D., Laforce, R.J., Masellis, M., Vandenberghe, R., Ber, I.L., Otto, M., van Minkelen, R., Papma, J.M., Rombouts, S.A., Balasa, M., Oijerstedt, L., Jelic, V., Dick, K.M., Cash, D.M., Harding, S.R., Jorge Cardoso, M., Ourselin, S., Rossor, M.N., Padovani, A., Scarpini, E., Fenoglio, C., Tartaglia, M.C., Lamari, F., Barro, C., Kuhle, J., Rohrer, J.D., Teunissen, C.E., van Swieten, J.C., 2016. Neurofilament light chain: a biomarker for genetic frontotemporal dementia. Ann. Clin. Transl. Neurol. 3, 623–636.
Meeter, L.H., Gendron, T.F., Sias, A.C., Jiskoot, L.C., Russo, S.P., Donker Kaat, L., Papma, J.M., Panman, J.L., van der Ende, E.L., Dopper, E.G.P., Franzen, S., Graff, C., Boxer, A.L., Rosen, H.J., Sanchez-Valle, R., Galimberti, D., Pijnenburg, Y.A.L., Benussi, L., Ghidoni, R., Borroni, B., Laforce Jr., R., del Campo, M., Teunissen, C.E., van Minkelen, R., Rojas, J.C., Coppola, G., Geschwind, D.H., Rademakers, R., Karydas, A.M., Öijerstedt, L., Scarpini, E., Binetti, G., Padovani, A., Cash, D.M., Dick, K.M., Bocchetta, M., Miller, B.M., Rohrer, J.D., Petrucelli, L., van Swieten, J.C., Lee, S.E., 2018. Poly(GP), neurofilament and grey matter deficits in *C9orf72* expansion carriers. Ann. Clin. Transl. Neurol. 15, 583–597.
Meeter, L.H., Kaat, L.D., Rohrer, J.D., van Swieten, J.C., 2017. Imaging and fluid biomarkers in frontotemporal dementia. Nat. Rev. Neurol. 13, 406–419.
Olson, I.R., Von Der Heide, R.J., Alm, K.H., Vyas, G., 2015. Development of the uncinate fasciculus: implications for theory and developmental disorders. Dev. Cogn. Neurosci. 14, 50–61.
Olszewska, D.A., Lonergan, R., Fallon, E.M., Lynch, T., 2016. Genetics of frontotemporal dementia. Curr. Neurol. Neurosci. Rep. 16, 107.
Onyike, C.U., Diehl-Schmid, J., 2013. The epidemiology of frontotemporal dementia. Int. Rev. Psychiatry 25, 130–137.
Papma, J.M., Jiskoot, L.C., Panman, J.L., Dopper, E.G., den Heijer, T., Donker Kaat, L., Pijnenburg, Y.A.L., Meeter, L.H., van Minkelen, R., Rombouts, S., van Swieten, J.C., 2017. Cognition and gray and white matter characteristics of presymptomatic C9orf72 repeat expansion. Neurology 89, 1256–1264.
Pereira, J.B., Ibarretxe-Bilbao, N., Marti, M.J., Compta, Y., Junque, C., Bargallo, N., Tolosa, E., 2012. Assessment of cortical degeneration in patients with Parkinson's disease by voxel-based morphometry, cortical folding, and cortical thickness. Hum. Brain Mapp. 33, 2521–2534.
Pievani, M., Paternico, D., Benussi, L., Binetti, G., Orlandini, A., Cobelli, M., Magnaldi, S., Ghidoni, R., Frisoni, G.B., 2014. Pattern of structural and functional brain abnormalities in asymptomatic granulin mutation carriers. Alzheimers Dement. 10 (5 Suppl), S354–S363.e1.
Rascovsky, K., Hodges, J.R., Knopman, D., Mendez, M.F., Kramer, J.H., Neuhaus, J., van Swieten, J.C., Seelaar, H., Dopper, E.G., Onyike, C.U., Hillis, A.E., Josephs, K.A., Boeve, B.F., Kertesz, A., Seeley, W.W., Rankin, K.P., Johnson, J.K., Gorno-Tempini, M.L., Rosen, H., Prioleau-Latham, C.E., Lee, A., Kipps, C.M., Lillo, P., Piguet, O., Rohrer, J.D., Rossor, M.N., Warren, J.D., Fox, N.C., Galasko, D., Salmon, D.P., Black, S.E., Mesulam, M., Weintraub, S., Dickerson, B.C., Diehl-Schmid, J., Pasquier, F., Deramecourt, V., Lebert, F., Pijnenburg, Y., Chow, T.W., Manes, F., Grafman, J., Cappa, S.F., Freedman, M., Grossman, M., Miller, B.L., 2011. Sensitivity of revised diagnostic criteria for the behavioural variant of frontotemporal dementia. Brain 134 (Pt 9), 2456–2477.
Renton, A.E., Majounie, E., Waite, A., Simon-Sanchez, J., Rollinson, S., Gibbs, J.R., Schymick, J.C., Laaksovirta, H., van Swieten, J.C., Myllykangas, L., Kalimo, H., Paetau, A., Abramzon, Y., Remes, A.M., Kaganovich, A., Scholz, S.W., Duckworth, J., Ding, J., Harmer, D.W., Hernandez, D.G., Johnson, J.O., Mok, K., Ryten, M., Trabzuni, D., Guerreiro, R.J., Orrell, R.W., Neal, J., Murray, A., Pearson, J., Jansen, I.E., Sondervan, D., Seelaar, H., Blake, D., Young, K., Halliwell, N., Callister, J.B., Toulson, G., Richardson, A., Gerhard, A., Snowden, J., Mann, D., Neary, D., Nalls, M.A., Peuralinna, T., Jansson, L., Isoviita, V.M., Kaivorinne, A.L., Holtta-Vuori, M., Ikonen, E., Sulkava, R., Benatar, M., Wuu, J., Chio, A., Restagno, G., Borghero, G., Sabatelli, M., Consortium, I., Heckerman, D., Rogaeva, E., Zinman, L., Rothstein, J.D., Sendtner, M., Drepper, C., Eichler, E.E., Alkan, C., Abdullaev, Z., Pack, S.D., Dutra, A., Pak, E., Hardy, J., Singleton, A., Williams, N.M., Heutink, P., Pickering-Brown, S., Morris, H.R., Tienari, P.J., Traynor, B.J., 2011. A hexanucleotide repeat expansion in C9ORF72 is the cause of chromosome 9p21-linked ALS-FTD. Neuron 72, 257–268.
Rohrer, J.D., Nicholas, J.M., Cash, D.M., van Swieten, J., Dopper, E., Jiskoot, L., van Minkelen, R., Rombouts, S.A., Cardoso, M.J., Clegg, S., Espak, M., Mead, S., Thomas, D.L., De Vita, E., Masellis, M., Black, S.E., Freedman, M., Keren, R., MacIntosh, B.J., Rogaeva, E., Tang-Wai, D., Tartaglia, M.C., Laforce Jr., R., Tagliavini, F., Tiraboschi, P., Redaelli, V., Prioni, S., Grisoli, M., Borroni, B., Padovani, A., Galimberti, D., Scarpini, E., Arighi, A., Fumagalli, G., Rowe, J.B., Coyle-Gilchrist, I., Graff, C., Fallstrom, M., Jelic, V., Stahlbom, A.K., Andersson, C., Thonberg, H., Lilius, L., Frisoni, G.B., Pievani, M., Bocchetta, M., Benussi, L., Ghidoni, R., Finger, E., Sorbi, S., Nacmias, B., Lombardi, G., Polito, C., Warren, J.D., Ourselin, S., Fox, N.C., Rossor, M.N., Binetti, G., 2015. Presymptomatic cognitive and neuroanatomical changes in genetic frontotemporal dementia in the Genetic Frontotemporal dementia Initiative (GENFI) study: a cross-sectional analysis. Lancet Neurol. 14, 253–262.
Rohrer, J.D., Ridgway, G.R., Modat, M., Ourselin, S., Mead, S., Fox, N.C., Rossor, M.N., Warren, J.D., 2010. Distinct profiles of brain atrophy in frontotemporal lobar degeneration caused by progranulin and tau mutations. Neuroimage 53, 1070–1076.
Rohrer, J.D., Warren, J.D., Barnes, J., Mead, S., Beck, J., Pepple, T., Boyes, R., Omar, R., Collinge, J., Stevens, J.M., Warrington, E.K., Rossor, M.N., Fox, N.C., 2008. Mapping the progression of progranulin-associated frontotemporal lobar degeneration. Nat. Clin. Pract. Neurol. 4, 455–460.
Rohrer, J.D., Warren, J.D., Fox, N.C., Rossor, M.N., 2013. Presymptomatic studies in genetic frontotemporal dementia. Rev. Neurol. (Paris) 169, 820–824.
Schonecker, S., Neuhofer, C., Otto, M., Ludolph, A., Kassubek, J., Landwehrmeyer, B., Anderl-Straub, S., Semler, E., Diehl-Schmid, J., Prix, C., Vollmar, C., Fortea, J., Deutsches, F.-K., Huppertz, H.J., Arzberger, T., Edbauer, D., Feddersen, B., Dieterich, M., Schroeter, M.L., Volk, A.E., Fliessbach, K., Schneider, A., Kornhuber, J., Maler, M., Prudlo, J., Jahn, H., Boeckh-Behrens, T., Danek, A., Klopstock, T., Levin, J., 2018. Atrophy in the thalamus but not cerebellum is specific for C9orf72 FTD and ALS patients - an atlas-based volumetric MRI study. Front. Aging Neurosci. 10, 45.

Schuster, C., Elamin, M., Hardiman, O., Bede, P., 2015. Presymptomatic and longitudinal neuroimaging in neurodegeneration–from snapshots to motion picture: a systematic review. J. Neurol. Neurosurg. Psychiatry 86, 1089–1096.
Seelaar, H., Rohrer, J.D., Pijnenburg, Y.A., Fox, N.C., van Swieten, J.C., 2011. Clinical, genetic and pathological heterogeneity of frontotemporal dementia: a review. J. Neurol. Neurosurg. Psychiatry 82, 476–486.
Seeley, W.W., 2010. Anterior insula degeneration in frontotemporal dementia. Brain Struct. Funct. 214, 465–475.
Shuter, B., Yeh, I.B., Graham, S., Au, C., Wang, S.C., 2008. Reproducibility of brain tissue volumes in longitudinal studies: effects of changes in signal-to-noise ratio and scanner software. Neuroimage 41, 371–379.
Smith, S.M., Jenkinson, M., Woolrich, M.W., Beckmann, C.F., Behrens, T.E., Johansen-Berg, H., Bannister, P.R., De Luca, M., Drobnjak, I., Flitney, D.E., Niazy, R.K., Saunders, J., Vickers, J., Zhang, Y., De Stefano, N., Brady, J.M., Matthews, P.M., 2004. Advances in functional and structural MR image analysis and implementation as FSL. Neuroimage 23 (Suppl 1), S208–S219.
Takao, H., Hayashi, N., Kabasawa, H., Ohtomo, K., 2012. Effect of scanner in longitudinal diffusion tensor imaging studies. Hum. Brain Mapp. 33, 466–477.
Takao, H., Hayashi, N., Ohtomo, K., 2013. Effects of the use of multiple scanners and of scanner upgrade in longitudinal voxel-based morphometry studies. J. Magn. Reson. Imaging 38, 1283–1291.
Turner, M.R., Agosta, F., Bede, P., Govind, V., Lule, D., Verstraete, E., 2012. Neuroimaging in amyotrophic lateral sclerosis. Biomark Med. 6, 319–337.
Uddin, L.Q., 2015. Salience processing and insular cortical function and dysfunction. Nat. Rev. Neurosci. 16, 55–61.
Van Mossevelde, S., van der Zee, J., Gijselinck, I., Sleegers, K., De Bleecker, J., Sieben, A., Vandenberghe, R., Van Langenhove, T., Baets, J., Deryck, O., Santens, P., Ivanoiu, A., Willems, C., Baumer, V., Van den Broeck, M., Peeters, K., Mattheijssens, M., De Jonghe, P., Cras, P., Martin, J.J., Cruts, M., De Deyn, P.P., Engelborghs, S., Van Broeckhoven, C., Belgian Neurology (BELNEU) Consortium, 2017. Clinical evidence of disease anticipation in families segregating a C9orf72 repeat expansion. JAMA Neurol. 74, 445–452.
van Swieten, J.C., Heutink, P., 2008. Mutations in progranulin (GRN) within the spectrum of clinical and pathological phenotypes of frontotemporal dementia. Lancet Neurol. 7, 965–974.
Walhout, R., Schmidt, R., Westeneng, H.J., Verstraete, E., Seelen, M., van Rheenen, W., de Reus, M.A., van Es, M.A., Hendrikse, J., Veldink, J.H., van den Heuvel, M.P., van den Berg, L.H., 2015. Brain morphologic changes in asymptomatic C9orf72 repeat expansion carriers. Neurology 85, 1780–1788.
Whitwell, J.L., 2010. Progression of atrophy in Alzheimer's disease and related disorders. Neurotox. Res. 18, 339–346.
Whitwell, J.L., Josephs, K.A., Avula, R., Tosakulwong, N., Weigand, S.D., Senjem, M.L., Vemuri, P., Jones, D.T., Gunter, J.L., Baker, M., Wszolek, Z.K., Knopman, D.S., Rademakers, R., Petersen, R.C., Boeve, B.F., Jack Jr., C.R., 2011a. Altered functional connectivity in asymptomatic MAPT subjects: a comparison to bvFTD. Neurology 77, 866–874.
Whitwell, J.L., Weigand, S.D., Gunter, J.L., Boeve, B.F., Rademakers, R., Baker, M., Knopman, D.S., Wszolek, Z.K., Petersen, R.C., Jack Jr., C.R., Josephs, K.A., 2011b. Trajectories of brain and hippocampal atrophy in FTD with mutations in MAPT or GRN. Neurology 77, 393–398.
Whitwell, J.L., Weigand, S.D., Boeve, B.F., Senjem, M.L., Gunter, J.L., DeJesus-Hernandez, M., Rutherford, N.J., Baker, M., Knopman, D.S., Wszolek, Z.K., Parisi, J.E., Dickson, D.W., Petersen, R.C., Rademakers, R., Jack Jr., C.R., Josephs, K.A., 2012. Neuroimaging signatures of frontotemporal dementia genetics: C9ORF72, tau, progranulin and sporadics. Brain 135 (Pt 3), 794–806.
Whitwell, J.L., Boeve, B.F., Weigand, S.D., Senjem, M.L., Gunter, J.L., Baker, M.C., DeJesus-Hernandez, M., Knopman, D.S., Wszolek, Z.K., Petersen, R.C., Rademakers, R., Jack Jr., C.R., Josephs, K.A., 2015. Brain atrophy over time in genetic and sporadic frontotemporal dementia: a study of 198 serial magnetic resonance images. Eur. J. Neurol. 22, 745–752.
Zhou, J., Greicius, M.D., Gennatas, E.D., Growdon, M.E., Jang, J.Y., Rabinovici, G.D., Kramer, J.H., Weiner, M., Miller, B.L., Seeley, W.W., 2010. Divergent network connectivity changes in behavioural variant frontotemporal dementia and Alzheimer's disease. Brain 133 (Pt 5), 1352–1367.